Soft Matter

PAPER

View Article Online
View Journal | View Issue

Cite this: *Soft Matter*, 2018, **14**, 1879

Fabrication of tough epoxy with shape memory effects by UV-assisted direct-ink write printing†

Kaijuan Chen,‡[ab] Xiao Kuang,‡[b] Vincent Li,[c] Guozheng Kang*[a] and H. Jerry Qi *[bc]

Received 1st December 2017,
Accepted 30th January 2018

DOI: 10.1039/c7sm02362f

rsc.li/soft-matter-journal

3D printing of epoxy-based shape memory polymers with high mechanical strength, excellent thermal stability and chemical resistance is highly desirable for practical applications. However, thermally cured epoxy in general is difficult to print directly. There have been limited numbers of successes in printing epoxy but they suffer from relatively poor mechanical properties. Here, we present an ultraviolet (UV)-assisted 3D printing of thermally cured epoxy composites with high tensile toughness *via* a two-stage curing approach. The ink containing UV curable resin and epoxy oligomer is used for UV-assisted direct-ink write (DIW)-based 3D printing followed by thermal curing of the part containing the epoxy oligomer. The UV curable resin forms a network by photo polymerization after the 1st stage of UV curing, which can maintain the printed architecture at an elevated temperature. The 2nd stage thermal curing of the epoxy oligomer yields an interpenetrating polymer network (IPN) composite with highly enhanced mechanical properties. It is found that the printed IPN epoxy composites enabled by the two-stage curing show isotropic mechanical properties and high tensile toughness. We demonstrated that the 3D-printed high-toughness epoxy composites show good shape memory properties. This UV-assisted DIW 3D printing *via* a two-stage curing method can broaden the application of 3D printing to fabricate thermoset materials with enhanced tensile toughness and tunable properties for high-performance and functional applications.

1. Introduction

3D printing has attracted increasing research interest in manufacturing due to some appealing features, such as design flexibility,[1–4] and its ability to realize complicated structures at high resolution.[5–7] Among the existing 3D printing techniques,[8,9] material extrusion is most widely used due to its cost-effectiveness and the wide choice of printable materials. For example, fused filament fabrication (FFF; or fused deposition modeling, FDM)-based 3D printing uses polymeric thermoplastic filaments, which can be extruded through a nozzle upon heating. Once exiting the nozzle, the filament cools down and the filament viscosity increases sharply, which rapidly holds the shape. With continuous filament deposition, the object is reconstructed in a layer-by-layer manner. Using this technique, a variety of thermoplastic polymers, such as ABS, PLA and PU, can be 3D printed. However, this conventional extrusion-based 3D printing method is limited to thermoplastic polymers and cannot be applied to chemically cross-linked thermosets.

Epoxy is one of the most widely used high-performance thermosetting polymers,[10] with applications in coating,[11,12] adhesives[13,14] and engineering structures[15,16] due to its outstanding properties, including high mechanical strength, thermal stability and chemical resistance. 3D printing of epoxy thermosets is highly desirable in high-performance applications, such as mechanical parts and aerospace, but remains a challenge. In the past, epoxy thermosets were directly printed using epoxy diacrylate *via* photo-induced radical polymerization or epoxy oligomer *via* UV light-induced cationic polymerization.[17] Although the high modulus and yield stress can be obtained, the strain at break is low at room temperature. In addition, the cationic initiators used in photocurable epoxy are more expensive, making them hard to use in large scale applications. As an alternative, other low-cost 3D printing technologies such as the direct-ink write (DIW) approach[18,19] have been developed to print thermally curable epoxy resin. In the work by Lewis' group,[19] the cellular structures (in a 2D pattern and with several layers in the thickness direction) were printed using epoxy composites ink reinforced by chopped carbon fibers and nanoparticles. In this approach, the ink containing the curable monomer or oligomer is extruded through a nozzle attached to a syringe

[a] *Applied Mechanics and Structure Safety Key Laboratory of Sichuan Province School of Mechanics and Engineering, Southwest Jiaotong University, Chengdu, Sichuan 610031, P. R. China. E-mail: guozhengkang@swjtu.edu.cn*
[b] *The George W. Woodruff School of Mechanical Engineering, Georgia Institute of Technology, Atlanta, GA 30332, USA*
[c] *School of Chemical and Biomolecular Engineering, Georgia Institute of Technology, Atlanta, GA 30332, USA. E-mail: qih@me.gatech.edu*

† Electronic supplementary information (ESI) available. See DOI: 10.1039/c7sm02362f

‡ These two authors contribute equally to this paper.

dispenser. The critical idea is that the ink viscosity is modified with nanoparticles to impart a shear-thinning effect, which enables a sharp decrease in viscosity at a high shearing rate and continuous ink extrusion. The filament can hold its shape due to the recovery of high viscosity after deposition. Followed by treating in an oven, the part is thermally cured into cross-linked thermosets. This cost-effective method can be applied to diverse resin systems. However, the thermal curing process needs to be carefully controlled and usually needs pre-curing at mild temperature to avoid deflection of the part. Since the viscosity of the part will decrease sharply at a high temperature, it may lead to shape distortion. Recently, Qian *et al.*[18] developed a method where they carefully controlled the pre-cure temperature and time to pre-crosslinking vitrimer epoxy resin so that they could print complicated 3D structures using the pre-cured vitrimer ink to create slight crosslinking to offer a high viscosity and to hold the shape even at a relatively mild temperature. However, the ink preparation is relatively tedious, which limits the wide adoption of this technique for 3D printing thermosets.

Recently, UV-assisted direct-ink-write fabrication was developed by Lebel *et al.*,[20] which enabled the *in situ* photo curing of a deposited filament. Upon the extrusion of the viscous photo curable ink at room temperature, UV curing enables instant cross-linking to fix the final polymerized shape. This approach has been successfully used to build continuous 3D-coiled geometries in a free-form fashion for functional applications, such as conductive spring coil and freestanding nanocomposite strain sensors.[20,21] In the same manner, this approach has been used to print glass and carbon fiber-reinforced dual-cure epoxy composites by Griffini and his coworkers.[22,23] Despite this advance in the *in situ* UV-assisted printing technique, there are still several challenges. First, the extrusion nozzle can be easily clogged since the photo-polymerization propagates to the nozzle due to the *in situ* cross-linking. Second, the mechanical properties of the 3D-printed thermosets are very brittle with a maximum fracture strain less than 3%, which limited their high-performance applications. Third, the mechanical properties are highly dependent on the printing parameters and anisotropic mechanical properties are observed because the interfacial strength between two adjacent layers determines the mechanical strength of the printed structures.[24]

To enable facile fabrication of high-performance epoxy thermosets with complex 3D structures, we report a new method of using the UV-assisted DIW technique *via* a two-stage cure. A new resin containing rapid photocurable resin and thermally curable epoxy oligomer is reinforced with fumed SiO_2, which can be utilized as ink for DIW printing. Each layer is printed followed by *ex situ* UV curing, which can efficiently avoid nozzle clogging. The flexible network formed by the UV curable resin can hold the shape of the part very well even at an elevated temperature. After DIW printing, the part with the complex structure is moved into a heating oven and thermally cured similar to conventional epoxy resin. Moreover, good interfacial bonding can be achieved by forming chemical bonds between different filaments leading to isotropic mechanical properties. This two-stage curing process enables the fabrication of interpenetrating polymer network (IPN) epoxy composites, which show high toughness with tunable mechanical properties. The printed epoxy composite also shows a good shape memory effect with a high shape fixity ratio, shape recovery ratio, and cycling stability.

2. Experimental sections

2.1 Materials and ink preparation

The DIW ink was prepared by mixing acrylate with epoxy resin of 4/6 (wt/wt) or about 17.6/18.2 (mol/mol). For the acrylate, *n*-butyl acrylate (BA, Sigma-Aldrich, St. Louis, MO, USA) was mixed with aliphatic urethane diacrylate (Ebecryl 8402, Alpharetta, GA. USA) at the BA/Ebecryl 8402 ratio of 1/1 (wt/wt) or about 15.6/2.0 (mol/mol). Bisphenol A diglycidyl ether (DGEBA) epoxy oligomer (Epon resin 862, Hexion Inc., Pueblo, CO, USA) was added into the acrylate. Then 1.5 wt% of 2,4,6-tris-dimethylaminomethyl phenol (Hexion Inc, Pueblo, CO, USA) as the curing agent, and 1.0 wt% of phenylbis(2,4,6-trimethylbenzoyl) phosphine oxide (Sigma-Aldrich, St. Louis, MO, USA) as the photoinitiator were added into the above mixture. Next, the mixture was mixed using a vortexer (Vortex-Genie 2, Bohemia, NY, USA) for five minutes. Finally, 8 wt% of fumed silica nanoparticle (Sigma Aldrich) was gradually added and stirred manually for 15 minutes. Before usage, the mixture was loaded into 10 cc, luer-lock syringes (Nordson EFD, Westlake, OH, USA) and centrifuged at 4000 rpm for 10 minutes to remove the bubbles.

2.2 The direct-ink write apparatus

The DIW printer setup was used for printing recyclable vitrimer epoxy,[18] PDMS(polydimethylsiloxane),[25] hydrogels[26] and conductive silver lines.[27] In this work, a photo-assisted DIW setup was developed as shown in Fig. S1 (ESI†). The syringe was controlled by a pressure regulator (Ultimus V, Nordson EFD, East Providence, RI, USA), which moved in the *x*- and *z*-directions, while the printing platform moved in the *y*-direction. A nozzle with 0.41 mm (22 GA) inner diameter was attached to the end of the syringe. A pressure of 33 psi and a printing speed of 10 mm s^{-1} were used during printing. It should be noted that the highest resolution can reach 250 μm by using a nozzle with an inner diameter of 250 μm in our printing system. In addition, our method can be used in other more advanced printing systems where a resolution as high as 20 μm could be achieved.[28] However, there is a balance between the resolution and printing efficiency for practical printing. The main limitation of our method is the relatively lower printing speed compared with other layer-based printing technologies, such as digital light processing (DLP). On the other hand, the DIW method has the advantages of excellent interfacial bonding between different filaments, and widely tunable mechanical properties after curing, which can be applied to a wide arrange of resins with high viscosity.

2.3 Material characterization

The rheology of mixtures was analyzed using a viscometer (DV3THB, Brookfield Engineering Labs Inc., Middleborough, MA, USA). The UV-differential scanning calorimetry (DSC, model Q2000,

TA Instruments, New Castle, DE, USA) tests were performed to study the photo curing reaction of the photopolymer in the printable ink under UV light by using a spot UV curing lamp (OmniCure S2000, Excelitas Technologies Corp., Waltham, MA, USA). Measurements were taken under a N_2 atmosphere at 25 °C with intermittent UV light. UV light at an intensity of 28 mW cm^{-2} was turned on for 10 s and off for 1 min each time. The on and off process was repeated until no reaction heat was observed. Fourier transform infrared spectroscopy (FTIR, Nicolet iS50, Thermo Fisher Scientific, Waltham, MA, USA) was used to monitor the reaction of the two-stage cure. An MTS tester (MTS Criterion™ Model 41, MTS Systems Corp., Eden Prairie, MN, USA) was used to test the uniaxial tensile mechanical properties at a strain rate of 1.5 mm min^{-1}. Dynamic mechanical analysis (DMA) was performed using a DMA tester (Model Q800, TA Instruments, New Castle, DE, USA). The detailed testing information can be found in the ESI†. Scanning electron microscopic (SEM) images were acquired on a Hitachi SU8010 SEM (Hitachi Ltd, Chiyoda, Tokyo, Japan).

3. Results and discussion

3.1 3D printing procedures for epoxy composites

The 3D printing procedure for epoxy composites is depicted in Fig. 1. In the first step, the filament was deposited for one layer on the platform through the DIW setup. In the second step, the platform was moved to a fixed position and then the UV lamp was turned on to photocure this layer for 10 seconds. After the second step, the platform moved back to the position under the DIW setup and a new layer was printed. By repeating these steps, a 3D object with complex shapes can be obtained. After printing, the obtained part was a chemically cross-linked elastomer that offered the necessary strength to hold the 3D-printed shape and also contained a large amount of epoxy oligomer that would be used for the second stage thermal cure. The part was then transferred into a hot oven for conventional thermal curing. The sample was pre-cured at 100 °C for 2 h and post-cured at 150 °C for 1 h. After that, the epoxy oligomer in the first network was polymerized to form an IPN with highly enhanced mechanical properties.

3.2 Characterization of ink

Our nanocomposite ink consisted of photo curable acrylates, thermally curable epoxy and fumed SiO_2 (200–300 nm particle). To facilitate DIW 3D printing, the shear-rate-dependent viscosity of the ink was measured using a viscometer as shown in Fig. 2a. The mixture without silica exhibited a nearly constant viscosity at a shear rate range from 1 s^{-1} to 500 s^{-1}, which can be taken as Newtonian behavior. When some amount of silica was added, a shear-thinning rheological behavior started to appear. With the addition of 8 wt% silica, an obvious shear-thinning behavior was obtained as the apparent viscosity decreased with increasing shear rate. This crucial property allowed the viscous composite ink to be extruded from the nozzle at high shear rates due to the drastic decrease in viscosity. After extrusion, the viscosity increased to a high level again after the ink was deposited, which prevented shape distortion prior to photo curing.

To determine the UV curing rate of the extruded material, a photo-DSC test was conducted. By measuring the heat generated during the curing reaction using DSC coupled with a UV-radiation source, the acrylate conversion or curing content in the ink with 40% weight fraction of photopolymer was evaluated. The test was conducted by shinning UV light for 10 second each time. As shown in Fig. 2b, the curing extent of the photopolymer reached 100% after 7 repeated UV irradiations until no heat was released.[17] It was observed that the curing extent reached about 80% after the first 10 seconds of UV irradiation, as shown in Fig. 2c. By balancing the printing efficiency and mechanical properties, a UV irradiation time of 10 seconds was chosen for each layer in our printing. It should be noted that the photocure reaction was almost not influenced by adding SiO_2 to the ink, see the DSC results in Fig. S2 (ESI†).

FTIR spectra were utilized to further confirm the curing reaction. As shown in Fig. 2d, the characteristic band of vinyl groups (δ^{ip}_{CH} = 1413 cm^{-1}) nearly disappeared after the first-stage UV curing (photo cure). After the second-stage cure (thermal cure), the epoxide groups (at 913 cm^{-1}) disappeared and hydroxyl groups (ν_{OH} = 3445 cm^{-1}) were generated. These results verified the formation of two different networks by different mechanisms yielding an IPN.[23] The schematical illustration of IPN is shown in Fig. S3 (ESI†).

3.3 3D printing epoxy composites

In order to demonstrate the printing behavior of the two-stage curing nanocomposite ink under the above-mentioned printing conditions (as shown in Fig. 1), a variety of complicated

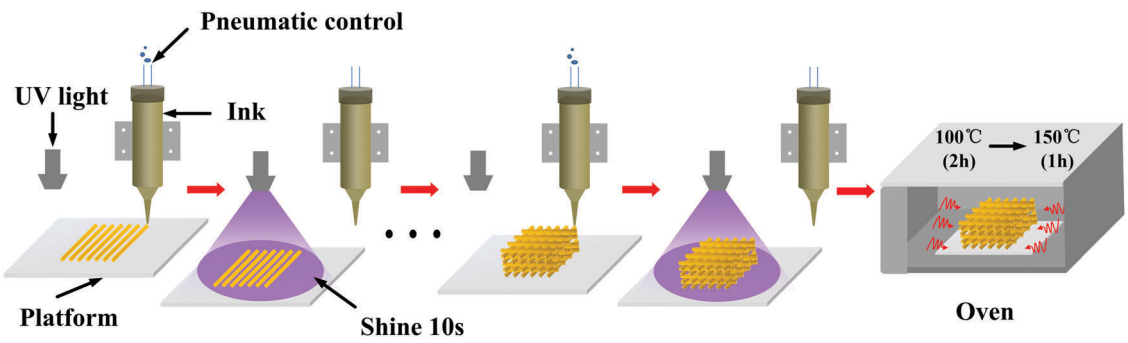

Fig. 1 Schematic illustration of the 3D printing epoxy composite material.

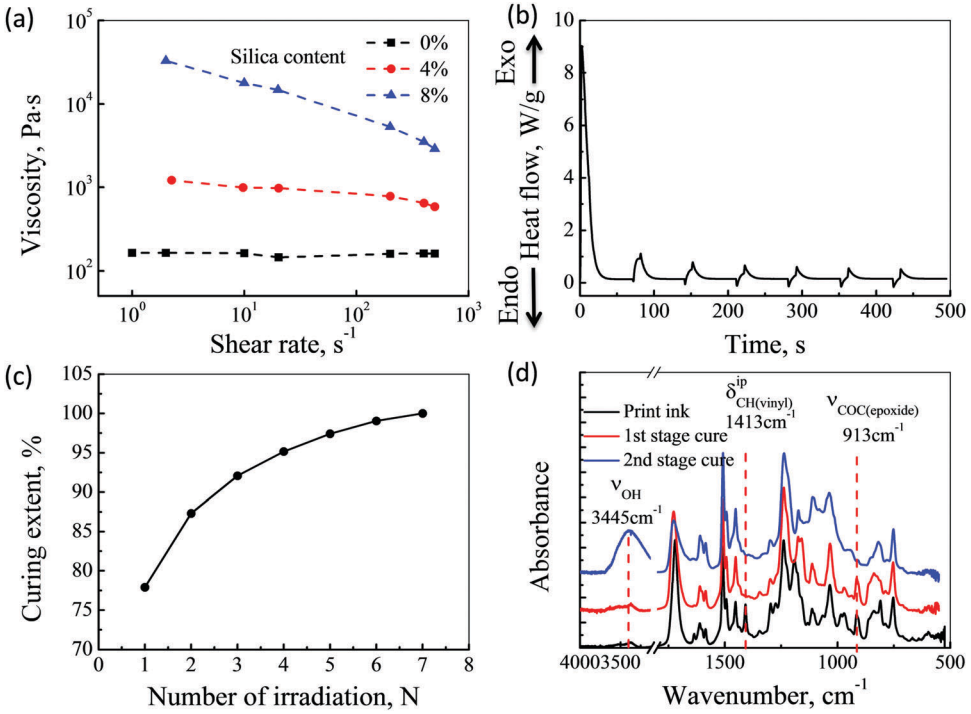

Fig. 2 (a) Viscosity curves of the epoxy composite resin with a different weight content of silica; (b) photo-DSC curve of the ink (epoxy composite resin with 8% silica); (c) curing extent of the ink as a function of the amount of irradiation; (d) FTIR spectra of the ink without cure, with 1st stage cure (photo cure) and 2nd stage cure (thermal cure).

architectures were printed using a 22 GA nozzle (0.41 mm inner diameter), as shown in Fig. 3. The images above the dashed line show the printed objects after the DIW 3D printing (Fig. 3a–d). The images under the dashed line show the objects after the 2nd stage thermal curing. Fig. 3a shows a square-shaped lattice structure, which is a 2D pattern composed of several layers that was able to maintain its shape well during the 2nd stage high temperature thermal cure. In addition to the lattice structure, complex structures with a micropattern, such as a gear wheel, were also printed. As shown in Fig. 3b, the spiral small gear teeth in the thickness direction were clearly visible. In addition, a spiral swirl bowl with a single-layered wall was successfully printed without any sagging and its dimension in the thickness direction was almost the same after thermal curing (from 18.43 mm to 18.39 mm), as shown in Fig. 3c. This confirms the excellent printability of the nanocomposite ink. Finally, a 3-links trophy object was printed (Fig. 3d; see Video 1 in ESI†) to show a comprehensive 3D printing ability. The microscale structure of the filament and printed structure were observed using SEM. Fig. 3(e) shows that the filament with a size of around 400 μm was clear without sagging. A close-up view of the filament shows its uniform dimensions. The filaments were tightly bound together since the thermal curing enables a polymerization reaction in the interfacial region. Such a feature provides an excellent interfacial adhesion between different layers.

3.4 Mechanical properties of the printed materials

The mechanical properties of the printing materials were evaluated using the uniaxial tensile tests. 3D printed epoxy composites with different printing paths were fabricated. Fig. S4a (ESI†) is the schematic illustration of the fabricated dog-bone shaped samples with different printing paths, *i.e.*, perpendicular to the stretching direction (0°), 45° to the stretching direction, and parallel to the stretching direction (90°). The printed samples with different printing paths are shown in Fig. S4b (ESI†).

Fig. 4a shows the representative stress–strain curves of the samples with 40% weight fraction of photopolymer with different printing paths. As a comparison, Fig. 4a also shows the stress–strain curves of the molded neat epoxy. It can be seen that the moduli of the neat epoxy and printed epoxy composite were around 1.92 GPa and 0.82 GPa; and the ultimate strains were about 5.3% and 25.4%, respectively, which showed the obvious enhanced tensile toughness. The tensile stress–strain curves of the printed samples with different printing paths nearly overlapped. Therefore, the mechanical properties of the printed epoxy composites, including Young's modulus and tensile strength, were insensitive to the printing path. These isotropic mechanical properties can be attributed to the excellent interfacial adhesion. It can be explained by two main factors: first, the liquid filament could be partially merged with the adjacent ones during printing, which could be bonded to each other after the UV curing; second, the thermal curing of the epoxy oligomer in the photo polymer provided additional adhesion, which could weld the filaments.

As discussed above, the printed IPN epoxy composites showed excellent mechanical properties, especially outstanding tensile toughness. To further evaluate the tensile toughness of

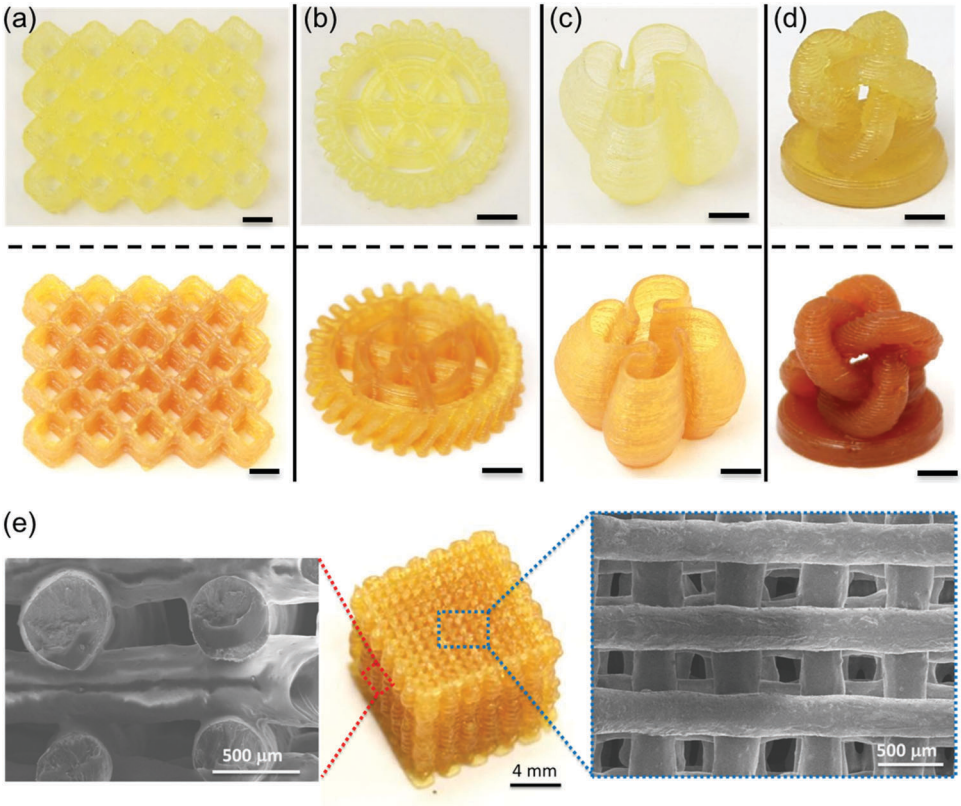

Fig. 3 Photo graphs and SEM images of the 3D printing with photo and thermal cure results of epoxy composites. The photos above the dashed line show the printed structures with the photo cure, and the photos under the dashed lines show the structures with two-stage cures (photo cure and subsequent thermal cure). (a) Square-shaped lattice structure; (b) gear wheel; (c) spiral swirl bowl; (d) 3-links trophy; (scale bars in a–d are 6 mm); (e) lattice structure with a single-layered wall and its enlarged SEM images.

the epoxy composites, the strain energy density (SED), *i.e.*, the area surrounded by the stress–strain curves, was used.[29,30] Fig. 4b shows that the SEDs of the printed IPN epoxy composites with different printing paths are similar (around 6 MJ m^{-3}). In addition, the SEDs of the IPN epoxy composites were nearly twice that of the mold neat epoxy. This indicates that the tensile toughness can be enhanced by the flexible photopolymer in the IPN composites. The fracture morphology observed using SEM also confirmed the enhanced tensile toughness of the IPN epoxy composites. As shown in Fig. 4c, the fracture surface of the neat epoxy was very smooth, indicating a typical brittle rupture. In contrast, the fracture surface of the printed IPN epoxy composites (with 0° printing path) was much rougher (Fig. 4d), which indicated that the IPN epoxy composites experienced large plastic deformation during the tension up to break. The plastic deformation accounted for the highly enhanced tensile toughness of the IPN epoxy composites, which originated from the incorporation of a flexible photo polymer.

Widely tunable mechanical properties of the IPN epoxy composites can be achieved by changing the weight fraction of the photopolymer, as shown in Fig. 4e and f. Fig. 4e shows the stress–strain curves for printed samples with different contents of acrylate and epoxy. It can be seen that the pure photo polymer was flexible but weak with a Young's modulus of 7 MPa and a fracture stress of 1.5 MPa, whereas the neat epoxy was strong and brittle. With the combination of these two materials, the IPN epoxy composites had enhanced tensile toughness with tunable mechanical properties, *i.e.*, modulus (1.31, 1.06 and 0.61 GPa) and ultimate strain (13.7, 18.1 and 32.1%) for 20, 30 and 40% weight fraction of photopolymer. It is noted that the IPN epoxy composites with 20, 30, and 40% weight fraction of photopolymer had much larger SED than those of the neat photopolymer and epoxy, as shown in Fig. 4f. Among them, the IPN epoxy composites with 40% weight fraction of photopolymer showed the largest failure strain and the highest SED. Furthermore, the glass transition temperature of the IPN epoxy composites can be tuned from 7.0 °C to 95.2 °C (Fig. S5, ESI†).

3.5 Shape memory effect

Shape memory effects in polymers have been explored in the past for a wide range of potential applications, such as biomedical devices,[31,32] aerospace engineering[33] and textiles.[34] The shape memory epoxy resins (SMERs) are attracting increasing attention due to their excellent shape memory properties.[35–37] The shape memory test activated by heat usually involves the following four steps. First, the sample is heated to above its transition temperature, such as the glass transition temperature (T_g), then is deformed under external load. Second, the

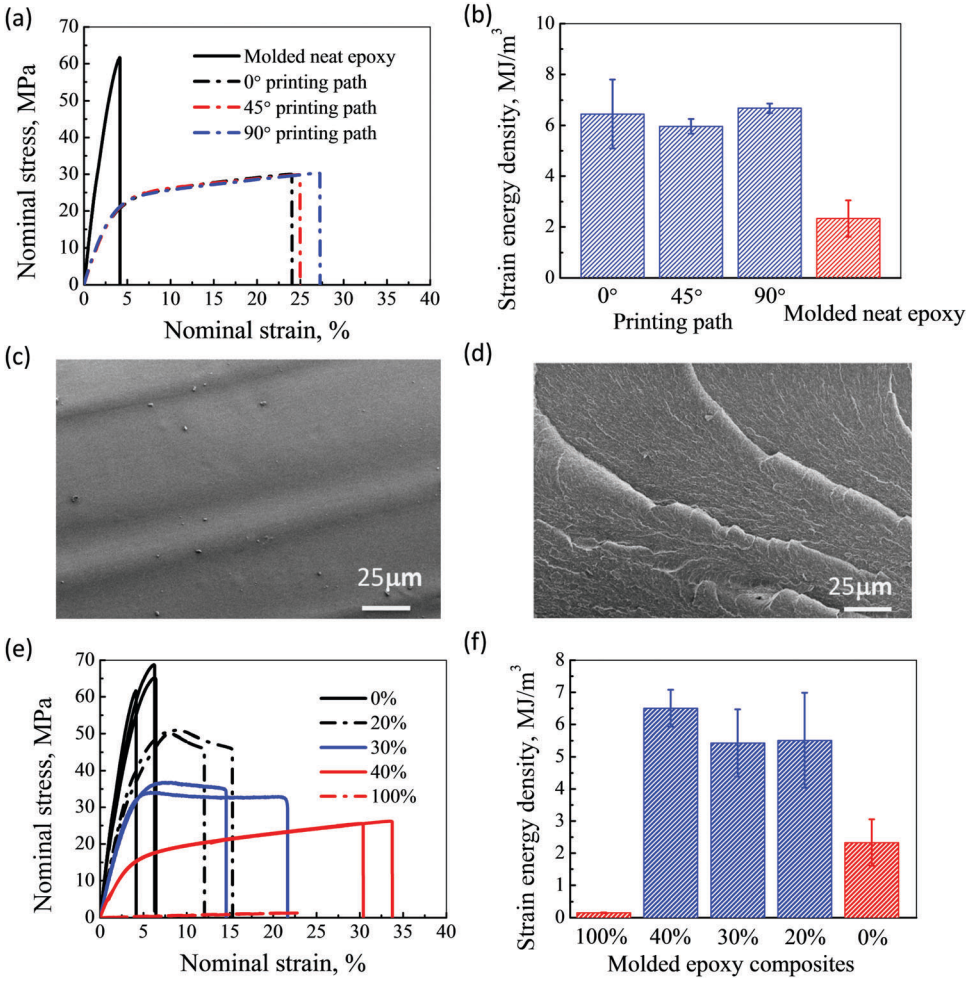

Fig. 4 (a and b) The stress–strain curves and strain energy density of the molded neat epoxy and print epoxy composites with different printing paths, respectively; (c and d) the SEM of the fracture surface of the molded neat epoxy and print epoxy composite material with 0° printing path, respectively; (e) and (f) the stress–strain curves and the strain energy density of molded epoxy composites with different weight fractions of photopolymer, respectively. Percentage is for the photocurable resin.

deformation is maintained, while the temperature is cooled to below T_g. Third, the external force is removed and the sample temporary shape is fixed. Finally, the sample is heated up to T_g again and it will recover its original shape.

Here, we used the epoxy composite with 40% weight fraction of photopolymer to demonstrate the shape memory effect. This composite had a T_g of 76.4 °C tested with DMA (Fig. S6, ESI†). The shape memory behavior was first demonstrated using a "GT" logo (Video 2, ESI†). From Fig. 5a, one can see that the shape recovery process of the deformed printed logo "GT" took about 10 seconds in a hot oil bath at a temperature of 104 °C (Fig. S7, ESI†). The shape memory effect was also demonstrated by the evolution of the opening angle for the strips. A printed strip sample (dimension: 35 mm × 5.0 mm × 0.8 mm) was deformed at 104 °C and the folded shape was fixed after cooling down. As shown in Fig. 5b, the folded strip gradually recovered to its original shape in a hot oil bath within 10 seconds, with rapid recovery in the first 5 seconds (81.1% recovery).

The DMA tester was used to quantitatively study the repeated shape memory properties of 3D printing epoxy composites, such as the shape fixity and shape recovery ratio. The sample was stretched to 10% at 110 °C and was then cooled down to 20 °C. The more detailed test process, and the definition of shape fixity ratio (R_f) and shape recovery ratio (R_r) are given in the ESI,† S8. It can be seen that the shape fixity ratio was about 97.1% for the repeated shape memory process. The shape recovery ratio was around 98.5% and was nearly the same in the subsequent shape memory cycles. The shape memory performance in our system is almost the same as Yu's work on the epoxy-acrylate hybrid photopolymer. It should be noted that the plastic deformation was observed in the first testing cycle, but it remained almost the same for the subsequent cycle, as shown in Fig. 5c. Similarly, this phenomenon was also observed by Yu *et al.*[17] on the epoxy-acrylate hybrid photopolymer due to the directional rearrangement of polymer chains under an external force.[38]

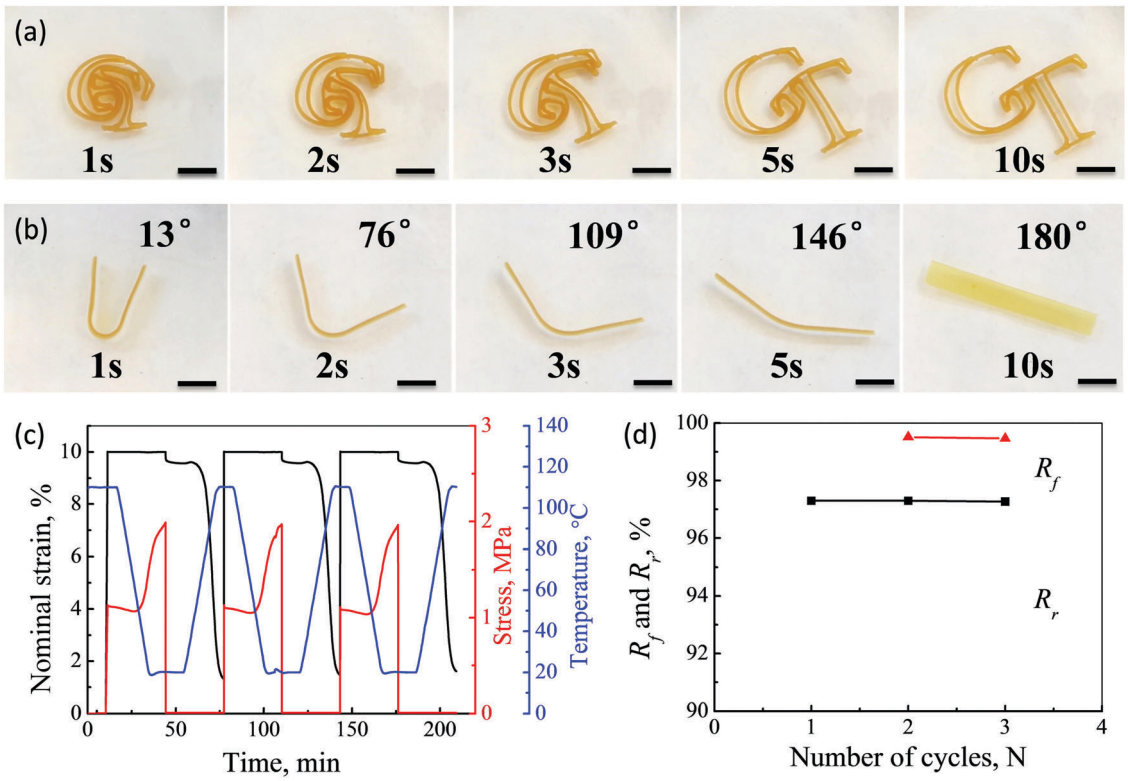

Fig. 5 The results of shape memory for printed samples; (a) and (b) the printing logo "GT" and strip sample in a 104 °C pump oil bath (scale bars in a and b are 8 mm); (c) stress, strain and temperature *vs.* time; (d) R_f and R_r *vs.* *N*.

4. Conclusion

We developed a new strategy for UV-assisted DIW 3D printing of thermally cured epoxy composites with high tensile toughness *via* a two-stage curing approach. The nanocomposite ink containing UV curable resin and an epoxy oligomer was used for direct-ink write (DIW)-based 3D printing followed by thermal curing. The shear-thinning effect enabled the successful extrusion of the filament and facilitated holding its shape after deposition in each layer. The UV irradiation induced photopolymerization and formed a crosslinked network to maintain the part's shape even at an elevated temperature. Followed by the 2nd stage thermal curing, an interpenetrating polymer network (IPN) epoxy composite with a complex 3D shape was obtained. This two-stage curing approach provides an excellent interfacial adhesion between filaments. The printed IPN epoxy composites also showed isotropic mechanical properties with highly enhanced tensile toughness. Moreover, the 3D-printed high-toughness epoxy composites exhibited good shape memory effects. With a wide choice of UV-curable resin, thermal curing resin and nanoparticles, this UV-assisted DIW 3D printing *via* a two-stage curing method can broaden the implementation of 3D printing to directly fabricate thermosetting materials with tunable and enhanced properties for high performance and functional applications.

Conflicts of interest

There are no conflicts to declare.

Acknowledgements

We gratefully acknowledge the support of an AFOSR grant (FA9550-16-1-0169; Dr B.-L. "Les" Lee, Program Manager) and the support of the NSF award (CMMI-1462895). A gift fund from HP, Inc, is also greatly appreciated. KC acknowledges support from the China Scholarship Council (No. 201607000069) as well as the Cultivation Program for the Excellent Doctoral Dissertation of Southwest Jiaotong University (No. D-YB201710).

References

1 D. Bak, *AsAut*, 2003, **23**, 340–345.
2 I. Gibson, D. Rosen and B. Stucker, *Additive manufacturing technologies: 3D printing, rapid prototyping, and direct digital manufacturing*, Springer, 2014.
3 K. Bootsma, M. M. Fitzgerald, B. Free, E. Dimbath, J. Conjerti, G. Reese, D. Konkolewicz, J. A. Berberich and J. L. Sparks, *J. Mech. Behav. Biomed. Mater.*, 2017, **70**, 84–94.
4 F. Yang, V. Tadepalli and B. J. Wiley, *ACS Biomater. Sci. Eng.*, 2017, **3**, 863–869.
5 Y. Mao, Z. Ding, C. Yuan, S. Ai, M. Isakov, J. Wu, T. Wang, M. L. Dunn and H. J. Qi, *Sci. Rep.*, 2016, **6**, 24761.
6 A. Cohen, A. Laviv, P. Berman, R. Nashef and J. Abu-Tair, *Oral Surgery, Oral Medicine, Oral Pathology, Oral Radiology, and Endodontology*, 2009, **108**, 661–666.

7 S. H. Ko, H. Pan, C. P. Grigoropoulos, C. K. Luscombe, J. M. Fréchet and D. Poulikakos, *Nanotechnol.*, 2007, **18**, 345202.
8 Y. Huang, M. C. Leu, J. Mazumder and A. Donmez, *Journal of Manufacturing Science and Engineering*, 2015, **137**, 014001.
9 Y. Jin, A. M. Compaan, W. Chai and Y. Huang, *ACS Appl. Mater. Interfaces*, 2017, **9**, 1820–1829.
10 Y. Xu and S. Van Hoa, *Compos. Sci. Technol.*, 2008, **68**, 854–861.
11 Z. Yu, H. Di, Y. Ma, Y. He, L. Liang, L. Lv, X. Ran, Y. Pan and Z. Luo, *Surf. Coat. Technol.*, 2015, **276**, 471–478.
12 D. Liu, W. Zhao, S. Liu, Q. Cen and Q. Xue, *Surf. Coat. Technol.*, 2016, **286**, 354–364.
13 J. Wernik and S. Meguid, *Mater. Des.*, 2014, **59**, 19–32.
14 X. Kuang, G. M. Liu, X. Dong, X. G. Liu, J. J. Xu and D. J. Wang, *J. Polym. Sci., Part A: Polym. Chem.*, 2015, **53**, 2094–2103.
15 J. Michels, R. Widmann, C. Czaderski, R. Allahvirdizadeh and M. Motavalli, *Composites, Part B*, 2015, **77**, 484–493.
16 M. B. Jakubinek, B. Ashrafi, Y. Zhang, Y. Martinez-Rubi, C. T. Kingston, A. Johnston and B. Simard, *Composites, Part B*, 2015, **69**, 87–93.
17 R. Yu, X. Yang, Y. Zhang, X. Zhao, X. Wu, T. Zhao, Y. Zhao and W. Huang, *ACS Appl. Mater. Interfaces*, 2017, **9**, 1820–1829.
18 Q. Shi, K. Yu, X. Kuang, X. Mu, C. K. Dunn, M. L. Dunn, T. Wang and H. J. Qi, *Mater. Horiz.*, 2017, **4**, 598–607.
19 B. G. Compton and J. A. Lewis, *Adv. Mater.*, 2014, **26**, 5930–5935.
20 L. L. Lebel, B. Aissa, M. A. E. Khakani and D. Therriault, *Adv. Mater.*, 2010, **22**, 592–596.
21 R. D. Farahani, H. Dalir, V. Le Borgne, L. A. Gautier, M. A. El Khakani, M. Lévesque and D. Therriault, *Nanotechnol.*, 2012, **23**, 085502.
22 M. Invernizzi, G. Natale, M. Levi, S. Turri and G. Griffini, *Materials*, 2016, **9**, 583.
23 G. Griffini, M. Invernizzi, M. Levi, G. Natale, G. Postiglione and S. Turri, *Polymer*, 2016, **91**, 174–179.
24 G. Postiglione, G. Natale, G. Griffini, M. Levi and S. Turri, *Polymer Composites*, 2017, **38**, 1662–1670.
25 M. Wehner, R. L. Truby, D. J. Fitzgerald, B. Mosadegh, G. M. Whitesides, J. Lewis and R. J. Wood, *Nature*, 2016, **536**, 451.
26 A. S. Gladman, E. A. Matsumoto, R. G. Nuzzo, L. Mahadevan and J. A. Lewis, *Nat. Mater.*, 2016, **15**, 413–418.
27 Q. Mu, C. K. Dunn, L. Wang, M. L. Dunn, H. J. Qi and T. Wang, *Smart Mater. Struct.*, 2017, **26**, 045008.
28 Z. J. Larimore, M. S. Mirotznik and P. E. Parsons, *2016 IEEE International Symposium on Antennas and Propagation (APSURSI)*, 2016, pp. 1937–1938.
29 Y. Zhao, B. H. Choi and A. Chudnovsky, *Int. J. Fatigue*, 2013, **51**, 26–35.
30 B. Jansen, S. Rastogi, H. Meijer and P. Lemstra, *Macromolecules*, 1999, **32**, 6290–6297.
31 A. Lendlein and R. Langer, *Science*, 2002, **296**, 1673–1676.
32 P. R. Buckley, G. H. McKinley, T. S. Wilson, W. Small, W. J. Benett, J. P. Bearinger, M. W. McElfresh and D. J. Maitland, *IEEE Trans. Biomed. Eng.*, 2006, **53**, 2075–2083.
33 Y. Liu, H. Du, L. Liu and J. Leng, *Smart Mater. Struct.*, 2014, **23**, 023001.
34 Y. Y. Chan Vili, *Text. Res. J.*, 2007, **77**, 290–300.
35 X. Kuang, G. Liu, X. Dong and D. Wang, *Polymer*, 2016, **84**, 1–9.
36 F. Castro, K. K. Westbrook, J. Hermiller, D. U. Ahn, Y. Ding and H. J. Qi, *J. Eng. Mater. Technol.*, 2011, **133**, 021025.
37 K. Yu, A. J. McClung, G. P. Tandon, J. W. Baur and H. J. Qi, *Mech. Time-Depend. Mater.*, 2014, **18**, 453–474.
38 T. Xie and I. A. Rousseau, *Polymer*, 2009, **50**, 1852–1856.

